

# A simple analytical model for dark matter halo structure and adiabatic contraction

E.A. Vasiliev

Lebedev Physical Institute, Moscow, Russia  
e-mail: eugvas@lpi.ru

A simple analytical model for describing inner parts of dark matter halo is considered. It is assumed that dark matter density is power-law. The model deals with dark matter distribution function in phase space of adiabatic invariants (radial action and angular momentum). Two variants are considered for the angular part of the distribution function: narrow and broad distribution. The model allows to describe explicitly the process of adiabatic contraction of halo due to change of gravitational potential caused by condensation of baryonic matter in the centre. The modification of dark matter density in the centre is calculated, and is it shown that the standard algorithm of adiabatic contraction calculation overestimates the compressed halo density, especially in the case of strong radial anisotropy.

PACS: 95.35.+d, 98.35.Ce, 98.35.Gi

## 1 INTRODUCTION

The structure and evolution of dark matter halos is widely discussed in the recent years (e.g. [1]) A large number of papers has been devoted to the investigation of spatial density profiles of dark matter halos,  $\rho(r)$ . both numerical [2, 3] and analytical [4]. Recently several papers appeared that described general properties of solutions of Jeans equation [5, 6]. The Jeans equation for a spherically symmetric self-gravitating system reads as follows:

$$\frac{d}{dr}(\rho \sigma_r^2) + \frac{2\beta}{r}(\rho \sigma_r^2) + \rho \frac{GM(r)}{r^2} = 0. \quad (1)$$

Here  $\sigma_r^2$  and  $\sigma_t^2$  are the radial and tangential velocity dispersion,  $\beta = 1 - \frac{\sigma_t^2}{2\sigma_r^2}$  is the Binney's anisotropy parameter (systems with  $0 < \beta < 1$  are radially anisotropic, with  $\beta < 0$  – tangentially anisotropic, and  $\beta = 0$  is the isotropic case).

An additional assumption is the following empirical property of dark matter halos: the generalized phase-space-*like* density of dark matter particles in a halo is a power-law in radius:

$$\rho(r)/\sigma_r^\epsilon(r) \propto r^{-\alpha}, \quad (2)$$

which is established both in N-body calculations [7] and some analytical models [6].

For a closed set of equations one also needs to specify  $\beta$ . Here two different approaches may be adopted: in [6] isotropy was assumed ( $\beta = 0$ ), and in [5] the following relationship between  $\beta$  and the logarithmic slope of density profile  $\gamma = d \ln \rho(r)/dr$  was taken:

$$\beta = \beta_0 + b(\gamma - \gamma_0). \quad (3)$$

This kind of relation has been proposed in [8] based on empirical analysis of different numerically treated situations.

These investigations demonstrated that under these assumptions there exist only few possibilities for a self-consistent halo model. The most realistic is the set of models with density profiles having inner and outer power-law asymptotes (so-called Zhao  $\alpha\beta\gamma$  models [9]).

However, this approach, being very fruitful, does not describe explicitly the distribution function. It operates only with its second moment with respect to velocity, i.e., the velocity dispersion. The most complete description of halo structure can be made in terms of phase-space distribution function  $f(r, v)$ . One attempt to deal with full velocity distribution function (VDF) was made in [10], where an Eddington inversion formula was applied to obtain VDF for power-law density profiles. However, this study was limited to isotropic case.

An approach based on certain physical assumptions regarding the form of the distribution function seems more promising. It avoids postulating empirical assumptions like (2, 3), which, nevertheless, still hold in many cases. It is convenient to express the distribution function in terms of adiabatic invariants during slow evolution of the gravitational potential. This allows to describe easily the process of adiabatic contraction of dark matter halo caused by condensation of baryonic matter in its centre, which occurs during the formation of a galaxy. This approach is adopted in the present paper.

The paper is organized as follows. In the second section we describe two models of inner halo structure and

explain physical arguments for the underlying assumptions concerning the dark matter distribution function. In the third section we calculate the velocity anisotropy coefficient. Furthermore, in the fourth section we consider the halo response to the adiabatic compression and compare it with other studies. Finally, the conclusions are presented.

## 2 THE PHASE-SPACE STRUCTURE OF MODEL HALO

Dark matter halos are extended complex objects which formed in different physical processes (growth of initial perturbations, collapse, hierarchical merging, and later – baryonic contraction). We are interested in the central area of a halo, which presumably is less influenced by merging and more – by condensation of baryons. Most of existing dark halo models assume power-law behaviour of density profile in the centre of a halo.

$$\rho_d(r) = K r^{-\gamma}, \quad 1 \leq \gamma < 2. \quad (4)$$

We shall adopt this assumption, having in mind that our analysis applies only to the inner area of a halo, interior to the radius where the logarithmic density slope starts to deviate from the constant value  $\gamma$ . The anisotropy coefficient is also taken to be constant in this area ( $0 \leq \beta < 1$ , according to analytical calculations and numerical simulations [11]). Under these assumptions,  $f$  depends on  $E$  also in a power-law form [12].

We write distribution function in terms of action-angle variables. The action variables are the angular momentum  $m$ , its projection onto  $z$  axis  $m_z$ , and radial action  $I_r$ , defined as  $I_r = \frac{1}{2\pi} \oint v_r(r) dr$ . The distribution function is quasi-stationary and hence does not depend on angle variables, and due to spherical symmetry, neither it depends on  $m_z$ . The radial action in power-law potential is well approximated by the following expression:

$$I_r = A E^{\frac{2-\gamma/2}{2-\gamma}} \left( 1 - \frac{m}{m_c(E)} \right), \quad (5)$$

where  $m_c(E)$  is the angular momentum of circular orbit with given energy [13].

We consider two variants of inner halo structure, which differ in the dependence of distribution function on angular momentum.

In the model A the angular momentum  $m$  of a particle is proportional its radial action:

$$m = l_0 I_r. \quad (6)$$

This relation, according to [14], emerges as a result of dynamical mixing in the centre of a collapsing dark matter halo. Initial density peak, which gives birth to the gravitationally bound object, is taken to be triaxial ellipsoid. Gravitational collapse and subsequent phase mixing, as shown in this paper, lead to formation of spherically symmetric structure, in which particles have angular momentum directly linked to their initial distance from centre, and, hence, with their radial action. The quantity  $l_0$  in expr. (6) is related to orbital eccentricity of particles:  $l_0 = 0$  corresponds to pure radial orbits, and  $l_0 \rightarrow \infty$  – to circular.

The distribution function in model A is expressed as follows:

$$f(I_r, m) = f_0 E^{1/2} \delta(m^2 - l_0^2 I_r^2). \quad (7)$$

In the model B the distribution function is given by expression

$$f(E, m) = f_0 E^\mu m^{-2B}, \quad \mu = \frac{1}{2} - \frac{4 - \gamma}{2 - \gamma} (1 - B). \quad (8)$$

This is the simplest generalization of isotropic model for the case of arbitrary radial anisotropy [12, 15].

Therefore, the two models considered represent, in some sense, two limiting cases – narrow and broad distribution by angular momentum for fixed energy. In what follows, we express particle energy through variables  $I_r$  and  $m$  according to (5), and rewrite the distribution function in action-angle variables.

Notice that we do not consider possible change of distribution function in the subsequent evolution, hierarchical clustering and merging, which is not significant for the inner parts of a halo, as shown in analytical calculations [16] and numerical simulations [17].

Due to scale invariance, the expression (2) is essentially satisfied, with  $\alpha = (1 - \frac{\gamma}{2})\epsilon$ . For  $\gamma < 2$  and  $\epsilon > 2$  the power-law index  $\alpha$  is slightly greater than 2. This is similar to ESIM (Extended Secondary Infall models) described in [6], in which the density has also power-law form at small radii.

## 3 VELOCITY ANISOTROPY

As long as the distribution function is given in action-angle variables, one can compute velocity distribution function at each radius, and, consequently, obtain radial and tangential velocity dispersion values  $\sigma_r^2$  and  $\sigma_t^2$ . Obviously, they should have also power-law form  $\sigma^2 \propto r^{2-\gamma}$ .

In the model A the anisotropy coefficient  $\beta$  is related to the density slope  $\gamma$  via the additional parameter  $l_0$  (see Fig.1). This relation can be approximated as

$$\beta \approx \gamma - 1 - 0.27 l_0 \gamma. \quad (9)$$

Hence, for a given  $l_0$  the relation between  $\gamma$  and  $\beta$  has linear form (3), though the coefficients differ from [8]. The upper bound on  $\beta$  equals  $\gamma - 1$ , in agreement with [18].

In the model B the anisotropy coefficient  $\beta$  is identical to B in expr. (8) [12]. Notice that it is possible to have  $\beta > \gamma - 1$ , if we recall that power-law density profile (4) breaks down at large radii. In this case the velocity dispersion is determined by density profile cutoff scale, and depends on radius as  $\sigma^2 \propto r^{\gamma-2\beta}$ . Upper bound on  $\beta$  is then  $\gamma/2$ , according to [15]. In the model A it is not possible, since it follows from expr. (5, 6) that the particle velocity at each radius lies in a limited range, proportional to  $\sqrt{\Phi(r)}$ , and hence, for sufficiently small radii the cutoff scale does not determine the velocity dispersion.

## 4 RESPONSE TO ADIABATIC CONTRACTION

It is well-known that central parts of galaxies are dominated by baryonic matter. The response of dark matter halo to the baryonic infall usually is calculated using the adiabatic approximation. The common algorithm for computing compression is that of Blumenthal et al. [19], in which dark matter particle's angular momentum is conserved. It is strictly applicable only to particles on circular orbits. In this method, the final radius  $r_f$  of a dark matter particle is related to its initial radius  $r_i$  by the following expression:

$$(M_{fin,DM}(r_f) + M_{fin,bar}(r_f)) r_f = M_{in,DM}(r_i) r_i, \quad (10)$$

where  $M_{fin,DM} + M_{fin,bar}$  is the total mass of dark matter and baryons after contraction, and  $M_{in,DM}$  is the initial dark matter mass inside a given radius.

In general case of non-circular orbits, the radial action is also conserved, being an adiabatic invariant. However, usually this does not help much, as the radial action is not known in general case. An improved method proposed in [20] involves the combination  $M(\bar{r}) r$ , where  $\bar{r}$  is the orbit-averaged radius of a particle. This yields less compressed halos, in better agreement with numerical simulations. Alternatively, an iterative method can be used for computing density profile and radial action in baryon-induced potential [21].

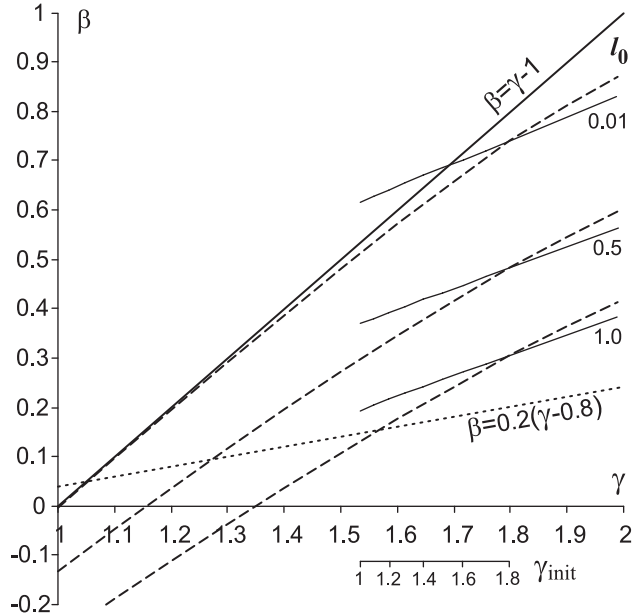


Figure 1: Anisotropy  $\beta$  vs. density slope  $\gamma$  relation in model A: dashed lines – initial anisotropy for different values of  $l_0$ ; solid lines – anisotropy after compression. Corresponding lines for the same  $l_0$  cross at  $\gamma = \Gamma = 1.8$ . Horizontal axis is the slope  $\gamma$  for original (uncompressed) halo and  $\gamma'$  for compressed, which depends on  $\gamma$  via (11). Corresponding original values of  $\gamma$  are shown in the bottom auxiliary axis. Thick line – upper limit  $\beta = \gamma - 1$ ; dotted line – Hansen & Moore relation [8]

In our simple models we are able to explicitly consider the adiabatic contraction, since we have our distribution function already written in terms of adiabatic invariants (provided that the characteristic timescale of the compression is much greater than dynamical timescale). All we need is to calculate radial action in new potential and recompute density profile. In many cases we may assume the baryonic density profile to be also power-law in radius:  $\rho_b(r) = K_B r^{-\Gamma}$ , with index  $\Gamma \leq 2$  (close to isothermal profile). This again applies only to central area of a galaxy, the bulge. We assume  $\Gamma > \gamma$ .

It is quite obvious that the modified dark matter density profile is also power-law:  $\rho'_d(r) = K' r^{-\gamma'}$ . The new power-law index  $\gamma'$  is expressed as follows:

$$\gamma' = \frac{3\Gamma + \gamma - \Gamma\gamma}{4 - \gamma}. \quad (11)$$

The power-law index is essentially the same as in Blumenthal's method, but the normalization coefficient is different. We introduce the quantity  $\eta = K'/K'_{std}$ , the

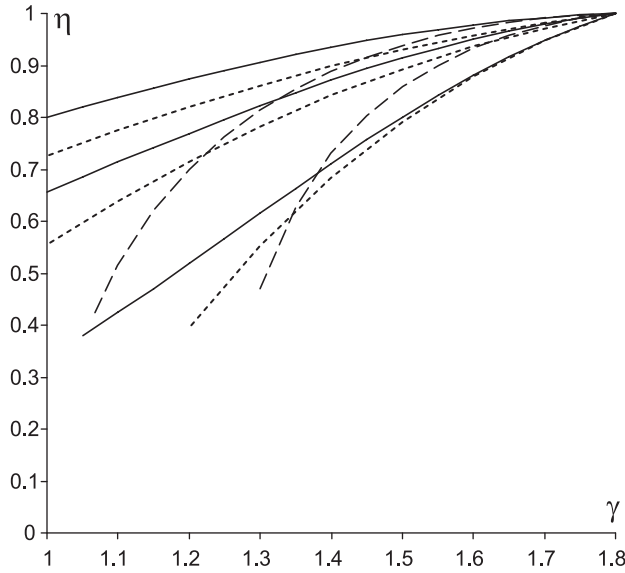


Figure 2:  $\eta$  – the ratio of our model’s density normalization to that of the standard adiabatic contraction model, for different values of anisotropy coefficient  $\beta$ . Dashed lines – model A,  $\beta = 0$  and 0.25 (from top to bottom); solid and dotted lines – models A and B correspondingly, for  $\beta = 0$ , 0.25 and 0.5 (top to bottom), in model A the anisotropy coefficient  $\beta'$  after contraction is used.

ratio of our model’s normalization to that of Blumenthal’s method (see Fig.2). It appears that  $\eta < 1$ , in agreement with the results of [20] and [21], where it was found that halos with radial motion are compressed less than predicted by Blumenthal et al. algorithm. The quantity  $\eta$  decreases with decrease in  $\gamma$  and increase in  $\beta$ . Numerical simulations in [22] also confirm this result; these authors explain it by the fact that for fixed  $\beta$  a greater value of  $\gamma$  increases the dominance of circular orbits over radial ones, and this makes Blumenthal’s method more applicable. (Note that when  $\beta$  tends to  $\gamma - 1$  in model A or to  $\gamma/2$  in model B, the density normalization is more and more affected by density cutoff radius, so that values of  $\eta$  are underestimated).

For quantitative calculations we take Milky Way bulge and dark halo as an example. The bulge density profile and normalization are taken from [23] and are the following:  $\rho_b = 0.6 \cdot 10^9 M_\odot/\text{kpc}^3 (r/1 \text{ kpc})^{-\Gamma}$ ,  $\Gamma = 1.8$ . The dark matter halo is normalized to have density 0.3 GeV/cm<sup>2</sup> at  $r=8.5$  kpc [24]. (Note that it yields different initial mass of dark matter inside 1 kpc, ranging from  $4 \cdot 10^8 M_\odot$  for  $\gamma = 1$  to  $3 \cdot 10^9 M_\odot$  for  $\gamma = 1.8$ . The baryonic mass within 1 kpc is  $6 \cdot 10^9 M_\odot$ ).

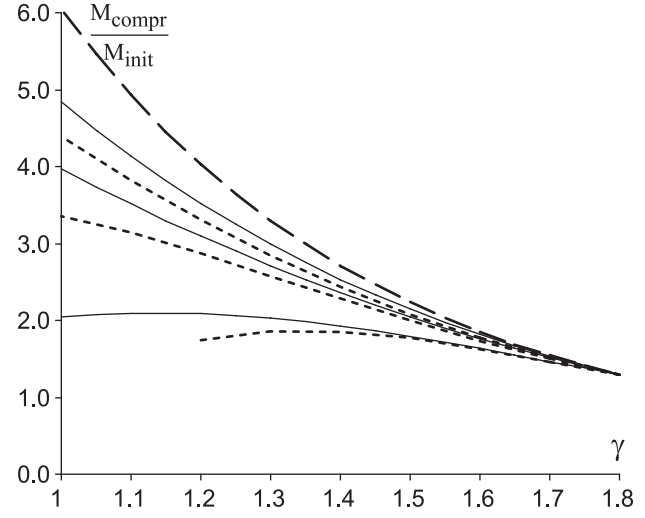


Figure 3: Ratio of compressed to initial dark matter mass within 1 kpc:  
long dashed – compressed by standard (Blumenthal) algorithm;  
solid and dotted lines – models A and B correspondingly, for  $\beta = 0$ , 0.25 and 0.5 (from top to bottom); in model A the anisotropy coefficient  $\beta'$  after contraction is used.

We calculate the ratio of new to old dark matter mass within radius 1 kpc and plot it in Fig.3. Again we see that with increasing  $\beta$  (more radial orbits), the actual compression ratio becomes smaller. The greater the difference between  $\gamma$  and  $\Gamma$ , the more is the increase in dark matter mass, i.e. the compression is more noticeable for halos with lower power-law index of initial density cusp.

And finally, we calculate the velocity anisotropy parameter  $\beta'$  for modified halo (see Fig.1). In model A it appears to be generally greater than for corresponding uncompressed halo, meaning that velocity becomes even more radially biased. At the same time, the relation between  $\beta'$  and  $\gamma'$  becomes more flat (the same effect can be seen from Fig.2 of [8] when comparing pure cosmological simulations and dark matter with cooling baryons simulations).

Having in mind that setting  $\Gamma = \gamma = \gamma'$  effectively does not change profile, we approximate velocity anisotropy parameter as

$$\beta' \approx \beta(\Gamma) + 0.4(\gamma' - \Gamma). \quad (12)$$

In model B the anisotropy coefficient slightly decreases (at most by 0.04 for  $\gamma = 1$ ,  $\beta = 0$ ). We note that due to increase in  $\beta'$  for model A it resembles more the model B in the reaction for adiabatic compression, if we plot the

compression coefficient as a function of  $\beta'$ , not  $\beta$  (solid and dashed lines in Figs.2 and 3).

## 5 CONCLUSION

We have considered two simple analytical models for structure of central part of dark matter halo. In both models, the distribution function depends on energy in a power-law form, and the dependence on angular momentum is  $\delta$ -function in model A and power-law in model B. The simplicity of the models allows us to calculate some interesting properties of the halo, namely: the velocity anisotropy and response to adiabatic contraction due to baryonic infall. These calculations help to get qualitative insight into halo properties and lead to the following conclusions:

1. The more radially biased is the velocity, the less compressed is the halo.
2. The shallower is initial density profile (less value of  $\gamma$ ), the less is the degree of compression compared to that of Blumenthal's method. Standard model of adiabatic contraction systematically overestimates the effect of contraction.
3. The model predicts a moderate enhancement (2 to 4 times) of dark matter mass in the bulge. The shallower is the initial profile, the greater the increase of dark matter mass. This result significantly increases the estimates of possible annihilation radiation flux from the center of the Galaxy [13, 24, 25].

I am grateful to Maxim Zelnikov for helpful discussion on the topic of the paper, to Steen Hansen for pointing out some interesting issues and to anonymous referee for valuable comments and proposals. This work was supported by Landau Foundation (Forschungszentrum Jülich) and Russian Fund for Basic Research (project nos. 01-02-17829, 03-02-06745).

## References

[1] G. Bertone, D. Merritt, *Mod.Phys.Lett. A* **20**, 1021 (2005).

[2] J. Navarro, E. Hayashi, C. Power et al., *MNRAS* **349**, 1039 (2004).

[3] J. Diemand, M. Zemp, B. Moore et al., *MNRAS* **364**, 665 (2005).

[4] Y. Lu, H. Mo, N. Katz, M. Weinberg, *MNRAS* (in press), astro-ph/0508624.

[5] W. Dehnen, D. McLaughlin, *MNRAS* **363**, 1057 (2005).

[6] C. Austin, L. Williams, E. Barnes et al., *Astrophys.J.* **634**, 756 (2005).

[7] J. Taylor, J. Navarro, *Astrophys.J.* **563**, 483 (2001).

[8] S. Hansen, B. Moore, *New Astron.* **11**, 333 (2006).

[9] H. Zhao, *MNRAS* **278**, 488 (1996).

[10] S. Hansen, D. Egli, L. Hollenstein, C. Salzmann, *New Astron.* **10**, 379 (2005).

[11] G. Mamon, E. Lokas, *MNRAS* **363**, 705 (2005).

[12] J. Binney, S. Tremaine, "Galactic Dynamics", Princeton Univ. Press (1987).

[13] P. Gondolo, J. Silk, *Phys.Rev.Lett.* **83**, 1719 (1999).

[14] A. Gurevich, K. Zybin, *Physics Uspekhi* **38**, 687 (1995).

[15] J. An, N. Evans, *Astrophys.J.* **642**, 752 (2006).

[16] W. Dehnen, *MNRAS* **360**, 869 (2005).

[17] S. Kazantzidis, A. Zentner, A. Kravtsov, *Astrophys.J.* **641**, 647 (2006).

[18] S. Hansen, *MNRAS* **352**, L41 (2004).

[19] G. Blumenthal et al., *Astrophys.J.* **301**, 27 (1986).

[20] O. Gnedin, A. Kravtsov, A. Klypin, D. Nagai, *Astrophys.J.* **616**, 16 (2004).

[21] J. Sellwood, S. McGaugh, *Astrophys.J.* **634**, 70 (2005).

[22] J. Choi, Y. Lu, H. Mo, M. Weinberg, *MNRAS* (submitted), astro-ph/0604587.

[23] V. Cardone, M. Sereno, *Astron. & Astroph.* **438**, 545 (2005).

[24] G. Bertone, D. Merritt, *Phys.Rev.D* **72**, 103502 (2005).

[25] M. Zelnikov, E. Vasiliev, *JETP Letters* **81**, No.3, 85 (2005).